



HAL
open science

Determination of the origin of the strength regain after self-healing of binary and ternary cementitious materials including slag and metakaolin

Carol Youssef-Namnoum, Benoit Hilloulin, Frederic Grondin, Ahmed Loukili

► To cite this version:

Carol Youssef-Namnoum, Benoit Hilloulin, Frederic Grondin, Ahmed Loukili. Determination of the origin of the strength regain after self-healing of binary and ternary cementitious materials including slag and metakaolin. *Journal of Building Engineering*, 2021, 41, pp.102739. 10.1016/j.jobbe.2021.102739 . hal-03537509

HAL Id: hal-03537509

<https://hal.science/hal-03537509>

Submitted on 20 Jan 2022

HAL is a multi-disciplinary open access archive for the deposit and dissemination of scientific research documents, whether they are published or not. The documents may come from teaching and research institutions in France or abroad, or from public or private research centers.

L'archive ouverte pluridisciplinaire **HAL**, est destinée au dépôt et à la diffusion de documents scientifiques de niveau recherche, publiés ou non, émanant des établissements d'enseignement et de recherche français ou étrangers, des laboratoires publics ou privés.

1 **Determination of the origin of the strength regain after self-healing of**
2 **binary and ternary cementitious materials**
3 **including slag and metakaolin**

4 Carol Youssef Namnoum, Benoit Hilloulin, Frederic Grondin*, Ahmed Loukili

5 *Institut de Recherche en Génie Civil et Mécanique (GeM), UMR 6183, Centrale Nantes –*
6 *Université de Nantes – CNRS, 1 rue de la Noë, 44321 Nantes, France*

7 e-mail: carol.youssef-namnoum@ec-nantes.fr; benoit.hilloulin@ec-nantes.fr;
8 frederic.grondin@ec-nantes.fr; ahmed.loukili@ec-nantes.fr

9 * Corresponding author: Tel.: + 33 (0) 2 40 37 68 47

10
11
12 **Highlights**

- 13 • Mechanical tests discriminate the healing performance of concretes
- 14 • XRD, TGA and SEM were employed to analyze the reaction products formed
15 during the healing process
- 16 • Ternary formulations with slag and metakaolin show better self-healing
17 performances
- 18 • Additional healing products are formed due to minerals additions in healed
19 cracks
- 20 • Microstructure of the healing products explain the global self-healing
21 performance

25 **Abstract**

26 A mechanical assessment of the self-healing process of complex cementitious materials
27 with mineral additions is presented. Mortars made with binary and ternary binders (blast
28 furnace slag, fly ash, metakaolin and silica fume) to reach 30 vol% substitution ratios
29 were prepared, and then small cracks with a width of 10 μm were created at the age of 2
30 days. After a 26-day healing period, mechanical properties obtained from three point
31 bending tests were analyzed to identify the recovery due to healing. In addition, the
32 microstructure of self-healing products was studied using various techniques (TGA,
33 SEM/EDS, and XRD). It was found that ternary compositions might exhibit a better self-
34 healing performance compared to single or binary compositions. The mechanical tests
35 indicate a better stiffness recovery for specimens prepared from the ternary mixture. This
36 improvement of mechanical response is presumably due to the newly formed products
37 precipitated in the cracks.

38
39 **Keywords:** self-healing; cementitious materials; minerals additions; mechanical
40 properties; microstructure; ternary compositions.

41
42 **1. Introduction**

43 In the actual context of climate change and the necessity to decrease greenhouse
44 emissions, the development of building materials with low content of cement has become
45 more relevant to reduce the civil engineering industry's carbon footprint. The use of latent
46 hydraulic or pozzolanic materials in place of clinker is one of the strategies discussed by
47 cement industry leaders and scientists. Besides, the deterioration of concrete structures
48 by time imposes enormous economic loss and environmental damage. Cracks, as a
49 damage sign, make it easier for harmful substances to penetrate into the concrete matrix

50 and thus reduce the durability of concrete structures. Therefore, a better characterization
51 of their properties and the prediction of their durability are important. In the last decade,
52 self-healing performance of concrete structures appears as a promising technique to
53 improve the durability and sustainability of a damaged structure by restoring its original
54 mechanical or permeability properties [1-3].

55 The intrinsic ability of concrete to heal is associated with the continuous hydration of
56 unhydrated cementitious particles and/or precipitation of calcium carbonate [4], [5].
57 When cracks occur in concrete structure and supplement water penetrates into the crack,
58 further hydration reactions take place owing to the presence of unhydrated cement
59 particles. This type of self-healing is called ‘autogenous healing’ process [6] where the
60 presence of water is essential to initiate the chemical reaction of the unreacted particles
61 of clinker. This healing process leads to secondary hydration products like C-S-H and
62 portlandite. The contact occurring between water and unhydrated particles of cement
63 induces the dissolution of Ca^{2+} and OH^- ions that start diffusing into the crack and
64 promotes the precipitation of new products around the crack. Following this mechanism,
65 the hydration products formed can re-establish the continuity of the material and improve
66 the mechanical properties of damaged concrete structure.

67 To highlight the self-healing efficiency, some researchers have adopted the visualization
68 (optical microscopy or X-ray microtomography technique) of crack filling as a direct test
69 to prove the continuous hydration [7]–[12]. Some other authors choose to indirectly
70 measure the recovery of matrix properties by means of mechanical tests [9], [10], [13]–
71 [15], durability tests such as air or water permeability [16]–[18] or nondestructive testing
72 [19].

73 It is generally considered that both stiffness and strength gains can be obtained after
74 two weeks of continuous immersion into water for 10 μm width crack [9], [16]. Moreover,

75 most of studies indicate that continued or cyclic immersion into water for several weeks
76 is needed to increase mechanical recovery. Others studies showed that healing potential
77 is highly improved when the crack is created at early age [5], [19]. The self-healing
78 properties vary according to the crack width, the type of binder [11], [12], [20], [21] and
79 the amount of unreacted cement grains in the concrete matrix [9], [13], [15], [21]–[23].
80 Studies showed that healing process is limited to a crack width smaller than 50 μm [14],
81 while others conclude that complete sealing (restoration of permeability) is also possible
82 for crack widths up to 200 μm [11]. While regarding mechanical properties, healing has
83 been reported as efficient for smaller width crack.

84 By now, several studies have been carried out to get more information about self-healing
85 by further hydration [7]–[12]. Concerning mechanical properties of healed cementitious
86 materials, experimental results reveal a possible strength recovery as well as a stiffness
87 recovery [13].

88 Moreover, it was found that using mineral additions could improve the autogenous self-
89 healing capabilities of concrete. By using mineral additions, an improvement of
90 permeability and strength of structure was observed compared to Portland cement that
91 has better mechanical properties at early age [11, 24–32,33]. These mineral additions lead
92 to change an ordinary cement paste to binary and ternary cementitious materials.

93 Recently, there is a great interest in using metakaolin as a supplementary cementitious
94 material in concrete. It is an ultra-fine material with strong pozzolanic activity, produced
95 by calcination of kaolin at temperatures between 700 and 900 $^{\circ}\text{C}$ [15]. Metakaolin consists
96 of silica and alumina product that react with portlandite to produce C-S-H gel and alumina
97 phases (C_2ASH_8 , C_4AH_{13} and C_3AH_6) [34]. Research results have shown that the use of
98 metakaolin is quite useful in improving the strength of concrete at a young age [36, 37],
99 or later [38, 39]. The combine use of slag and metakaolin have an influence in enhancing

100 mechanical properties and durability of mortar and concrete. The highly active pozzolanic
101 reaction of metakaolin with respect to the latent hydraulic properties of slag can explain
102 this equilibrium of functions leading to improved mechanical behaviour, where the
103 presence of both materials have no adverse effect [38]. This enhanced performance is due
104 to the filler effect which improve the microstructure density [39] and the diversity of
105 hydration products formed from a ternary mixture containing metakaolin and slag, like
106 C_2ASH_8 , C_4AH_{13} and C_3AH_6 [39]. Mohammadi et al. [40] have recently shown the
107 interest to combine formulations and other mineral additions on the self-healing capacity
108 regarding the variety of the self-healing products.

109 In spite of the benefits of using mineral additions, few tests have been performed in order
110 to investigate their role on the mechanical properties through the self-healing process.
111 Salama et al. [27] reported that the highest recovery in mechanical and permeability
112 properties was obtained with cement composites incorporating 25% of slag and with the
113 mixtures containing metakaolin, which behaves very similarly to the ordinary mixture
114 containing 100% cement. Termkhajornkit et al. [38] reported that increasing the fly ash
115 content leads to an increasing of the self-healing efficiency by measuring the amount of
116 chloride ions diffused before and after self-healing. Erdoğan Özbay and Sahmaran [39]
117 assessed the healing performance of fiber concrete ECC containing fly ash. The results
118 show a better healing performance when the CaO content is higher.

119 With the increasing development of ternary formulations motivated by economic and
120 environmental considerations in the first place, it is important to understand what happens
121 during the self-healing phenomenon. The development of ternary formulations favorable
122 to healing could be useful for on-site industrial applications. Research works have mainly
123 focused on characterizing self-healing properties for binary blends of concrete materials
124 regarding permeability regains, and very little work has been carried out on the

125 microstructure and durability of concrete incorporating various mineral admixtures. In
126 particular, the effect of using both slag and metakaolin on the mechanical performance of
127 healing process has never been reported in the literature to our knowledge.
128 This paper presents an experimental study on the chemo-mechanical characterization of
129 the self-healing phenomenon of cementitious materials with low content of cement
130 including supplementary cementitious materials. Therefore, a complete study has been
131 performed to highlight the best binder mixture regarding the self-healing capacity. The
132 mineralogy of the self-healing products in cracks of various cement pastes including
133 SCMs was investigated with scanning electron microscope equipped with an energy
134 dispersive spectroscopy (EDS), thermogravimetric analysis (TGA) and X-ray diffraction
135 test (XRD). Artificial gaps were designed to obtain the powders of healing products in
136 order to distinguish the newly formed reaction products from the bulk paste [10]. In
137 addition, the influence of the mix design on the potential of self-healing was studied. 2D
138 microscope measurements were performed before and after healing to indicate the
139 processing of self-healing phenomenon. The mechanical behaviour of pre-cracked
140 mortars containing SCM subjected to healing was assessed by means of three points
141 bending tests to quantify the regains of mechanical properties.

142

143 .

144

145 **2. Materials and methods**

146 **2.1 Materials**

147 In this study, mortars were prepared with materials used to have beneficial effects on
148 healing potential. All mortars mixtures were prepared with ordinary Portland cement
149 (CEM I 52.5 N), SAREMER sea sand 0/4, the same paste volume 530 l/m^3 and the same

150 water-to-binder ratio of 0,4. Different supplementary cementitious materials (SCM) like
 151 Metakaolin (MK), Slag (S), Fly Ash (FA) and Silica Fume (SF) were used as partial
 152 volume substitution of cement up to 30%. Chemical compositions and physical properties
 153 are detailed in **Erreur ! Source du renvoi introuvable.** C₁₀₀ was considered as the
 154 ordinary mixture made with only Portland cement (100% of cement). Binary (C_xA_y),
 155 ternary (C_xA_yB_z), mixtures were made with x% of cement (C_x) and y% of SCM,
 156 respectively y% and z% of SCM = {MK, S, FA, SF}. The mixture design of all mortars
 157 prepared for this study is summarized in Table 2.

158 **Table 1.** Chemical composition and properties of Portland cement and additions used in
 159 this study.

		Cement	Metakaolin	Slag	Fly ash
Chemical composition (%)	SiO₂	19,6	93,16	37,7	50
	Al₂O₃	4,5		10,2	8,5
	Fe₂O₃	2,3	-	0,6	29
	CaO	63,7	0,36	43,8	2,15
	MgO	3,9	0,04	6,4	-
	SO₃	2,6	-	0,1	0,37
Physical properties	Specific gravity (Kg / m³)	3130	2500	2900	2100
	Specific area (m²/g)	0,39	16	0,45	0,23

160

161 **Table 2.** Mortars mixtures

	w/b	Sea Sand 0/4 (kg/m ³)	Binders content (vol%)
C ₁₀₀	0,4	1231	0
C ₇₀ MK ₃₀	0,4	1231	30% MK
C ₇₀ S ₃₀	0,4	1231	30% S
C ₇₀ SF ₃₀	0,4	1231	30% SF
C ₇₀ FA ₃₀	0,4	1231	30% FA
C ₇₀ MK ₁₅ S ₁₅	0,4	1231	15% MK + 15% S

162

163 **2.2 Samples preparation for the assessment of mechanical regains due to self-healing**

164 For the determination of the compressive strength of mortars mixtures, three $4 \times 4 \times 16 \text{ cm}^3$
165 specimens of each mixture were tested at 2, 7 and 28 days, according to European
166 standard protocol EN 12 390-3. For binary and ternary mixtures, activity index R was
167 presented as the ratio between the compressive strength of the mortar with mineral
168 addition (f_i) and the compressive strength of the ordinary mixture mortar C_{100} (f_0) : $R = f_i$
169 / f_0 .

170 In order to study the effect of healing process on mechanical properties of these different
171 mixtures, mortar prisms of dimensions $7 \times 7 \times 28 \text{ cm}^3$ and $4 \times 4 \times 16 \text{ cm}^3$ were prepared.
172 Specimens were vibrated into two layers on a horizontal vibrating table in order to
173 minimize the amount of occluded air. After 24 hours of curing under sealed conditions in
174 a room at $20 \text{ }^\circ\text{C}$ and 85-95% relative humidity, the specimens were demolded. A notch
175 was cut at the middle of $7 \times 7 \times 28 \text{ cm}^3$ specimens with a depth of 7 mm and thickness of
176 5 mm by means of precision saw machine, in order to initiate cracking at a specific
177 location using three-point bending test. Following that, specimens were stored in tap
178 water at $20 \text{ }^\circ\text{C}$ before cracking and during the healing period. Two prepared samples of
179 each mixture were pre-cracked at the age of 48 hours by three-point bending test whereas
180 the crack mouth opening displacement (CMOD) was controlled with a constant rate of
181 $0,2 \text{ }\mu\text{m/s}$, following ASTM C78 norm. The aim of this step was to obtain a residual crack
182 width equal to $10 \text{ }\mu\text{m}$, which permits to get a fast healing process. The choice of an initial
183 width-crack of $10 \text{ }\mu\text{m}$ created at the age of 48 hrs is related to better mechanical regains
184 obtained for specimens cracked at a young age as revealed by [41]. The real crack width
185 was measured using a 2D microscope. Then, the specimens were further cured in tap
186 water $20 \text{ }^\circ\text{C}$ under unsealed condition.

187 . After healing for 26 days, the healed and the reference specimens were reloaded after 1-
188 h exposure to room temperature necessary for the Crack Mouth Opening Displacement

189 (CMOD) dispositive preparation. The drying time is chosen to be as short as possible to
 190 avoid alteration of the healing products. The healing phenomenon was verified by 2D
 191 microscopic observations that show the precipitations of newly formed healing products.
 192 By employing three-point bending test, three prisms specimens from each mixture were
 193 reloaded in order to characterize the residual mechanical properties after healing process.
 194 These three specimens consist of two samples pre-cracked and healed while the third one
 195 represents the reference sample (un-cracked before curing). At this step, a flexural stress-
 196 deflection curve obtained when the healed samples were mechanically reloaded is
 197 compared to the loading curves of the reference sample having undergone the same curing
 198 conditions [31], [41].
 199 The performance of healing was quantified by using two equations 'format of mechanical
 200 regains related to strength and stiffness recovery respectively [31]:

$$IR.strength = \frac{F_{healed} - F_{unhealed}}{F_{ref} - F_{unhealed}} \quad (1)$$

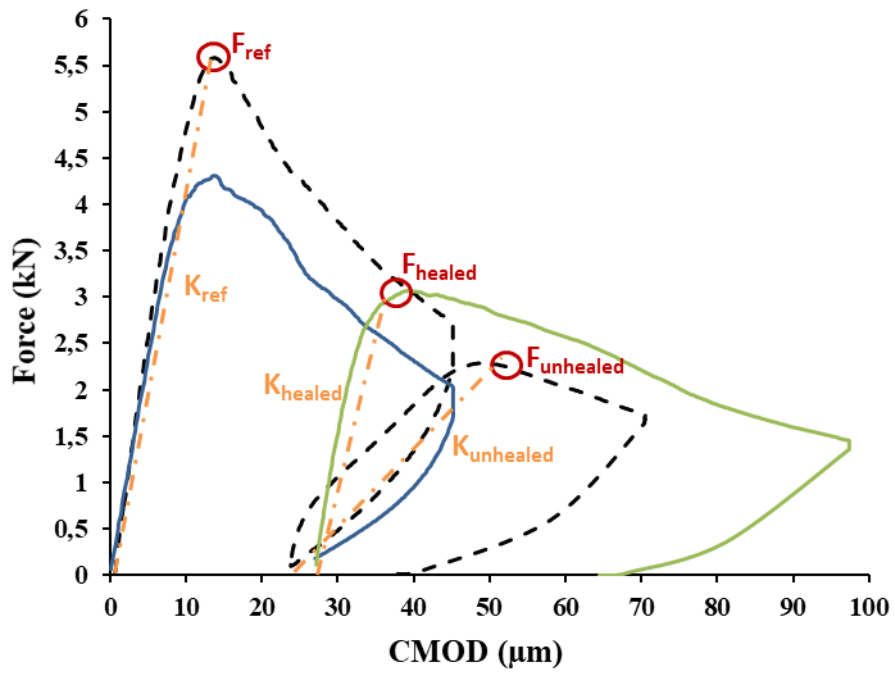
$$IR.stiffness = \frac{K_{healed} - K_{unhealed}}{K_{ref} - K_{unhealed}} \quad (2)$$

201
 202 where F_{healed} represents the maximum strength of the healed samples during reloading,
 203 F_{ref} the maximum strength of reference sample loaded at 28 days, $F_{unhealed}$ the reloaded-
 204 maximum strength of reference sample, K_{healed} the maximum stiffness of the healed
 205 samples during reloading, K_{ref} the maximum stiffness of reference sample and $K_{unhealed}$
 206 the reloaded-maximum stiffness of reference sample. K values were calculated by
 207 drawing a tangent on the loaded and reloaded curve. These two indexes vary between 0
 208 (no healing) and 1 (total healing). The different elements of indexes are represented in
 209 Fig.1. The overall program for three point bending test after 4 weeks of age is presented
 210 in Fig.2.

211
 212

213

214

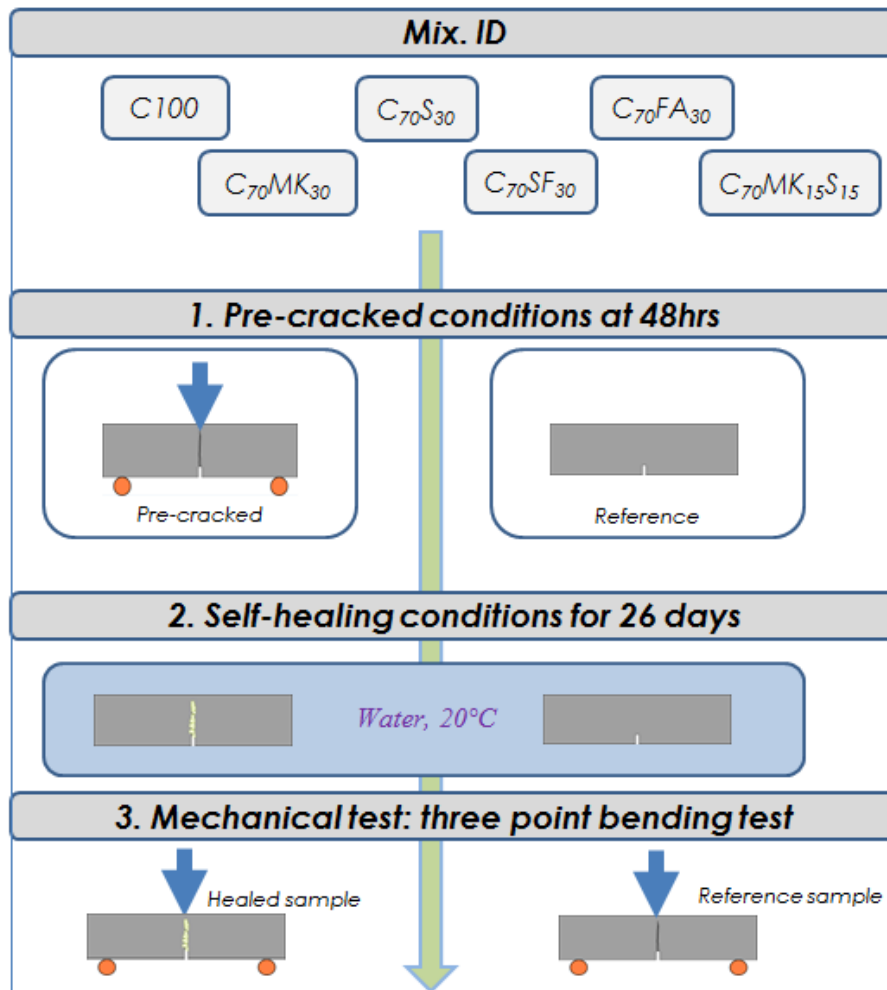


215

216 **Fig.1** Example of Load vs. CMOD curves for specimens submitted to healing and
217 reference specimens; representation of quantities for calculation of self-healing indexes.

218

Authors



219

220 **Fig.2** The experimental program flowchart adapted to identify the performance of self-
 221 healing.

222

223 2.3 Morphology of self-healing products: testing procedures

224 The characterization of reaction products formed in healing process has been performed
 225 by using different tests 'SEM/EDS, TGA, XRD analyses. A special procedure consisted
 226 of the creation of artificial cracks was followed [10]. First, 4×4×16 cm³ cement paste
 227 samples were prepared from the different mortars formulations mentioned before. Then,
 228 the samples were demolded after 24 hours of curing in room at 20°C and 90± 5% relative
 229 humidity.

230 At 48 hours, the specimens were sliced into dimensions of 4 cm height, 4 cm length and
 231 1 cm thickness. A total of 16 slices was obtained per 1 specimen. Following that, the 16

232 slices were pressed together by using a plastic clamp and immersed in tap water for 4
233 weeks (Fig.3 **Erreur ! Source du renvoi introuvable.**). The gap width between the slices
234 does not exceed the 30 μm . It was measured by a microscope. During the healing process,
235 new reaction products were precipitated inside the artificial planar gaps between two
236 slices. After the self-healing period, the cement paste slices were separated and vacuum-
237 dried during 2h. The slices have been observed by SEM equipped with EDS to determine
238 the morphology of healing products formed between each two flat slices and their
239 chemical structures.

240 In addition, the healing products were scratched off easily from the slice surfaces by using
241 an aluminum spatula then powders obtained were tested. Besides, the internal part of
242 cement paste matrix were grounded into powder and tested in order to differentiate the
243 primary hydrate phases from the healed products formed between the slices. Analysis of
244 mineralogy was performed on these fine powders using TGA and XRD tests. As
245 mentioned in [10], the planar gaps have no influence on the chemical natures of the
246 healing products formed by further hydration.

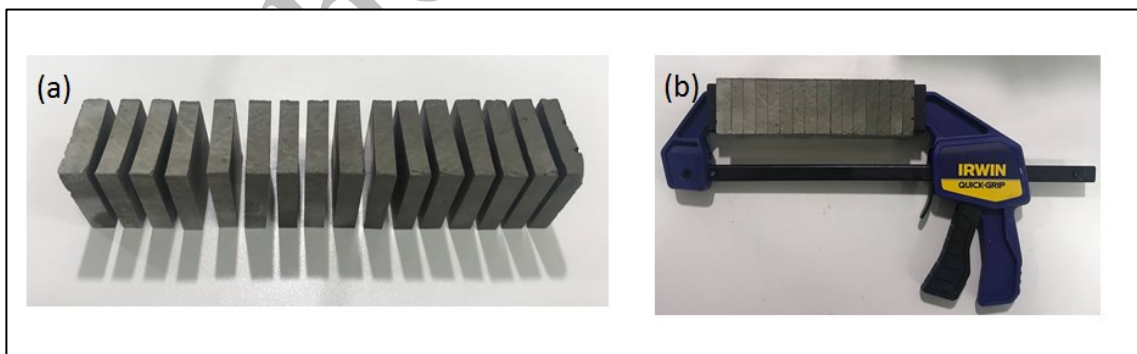


Fig.3 Slices cut from 40x40x160 mm cement paste specimen (a), slices pressed together using a clamp (b).

247 **2.3.1 SEM / EDX**

248 The microstructure of products formed in planar gaps was observed via scanning
249 electronic microscopy (SEM) coupled with EDS in order to get more information on

250 chemical elements of the reaction products. The microscopic analysis technic used was a
251 scanning electron microscope JEOL JSM-6060LA, used at a distance of 9-11mm for
252 pictures, and an acceleration voltage of 20kV to acquire high contrast images. It was
253 equipped by an EDS detector. The slices observed were placed into vacuum under a
254 pressure of 60Pa into the SEM.

255

256 **2.3.2 TGA**

257 Thermogravimetric measurements (TGA) were performed in nitrogen atmosphere at 0.6
258 bars by using a Netzsch STA 449 F3 Perseus device. The studied materials were crushed
259 to obtain 50 mg samples. The heating rate was 20 °C/min and the highest temperature
260 applied was 1400°C.

261

262 **2.3.3 XRD**

263 After healing for 26 days, X-ray diffraction (XRD) measurements were performed on a
264 Bruker D8 phaser instrument. Scans were conducted with a step size of 2.5°, for 0.1 s per
265 step while 2θ range between 5° and 60°. Analysis was carried out by using Eva software.

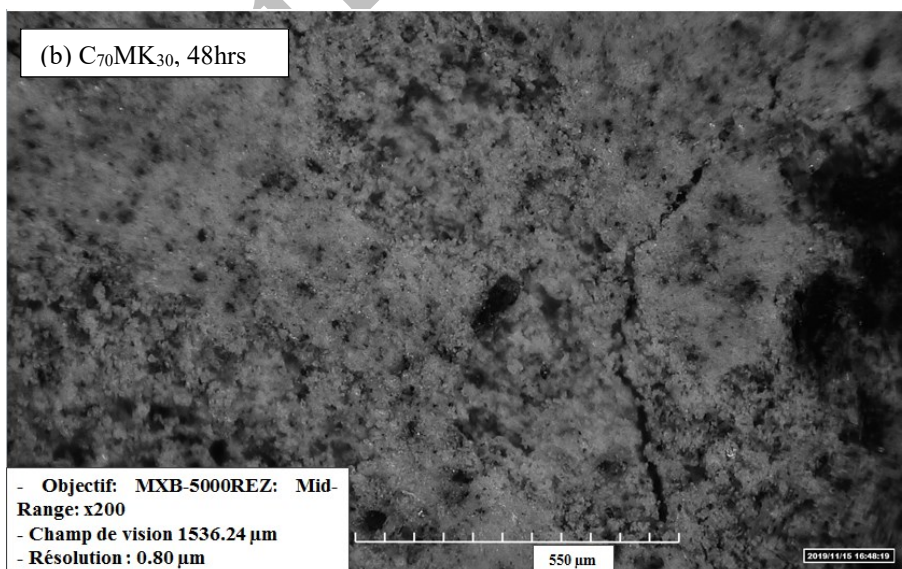
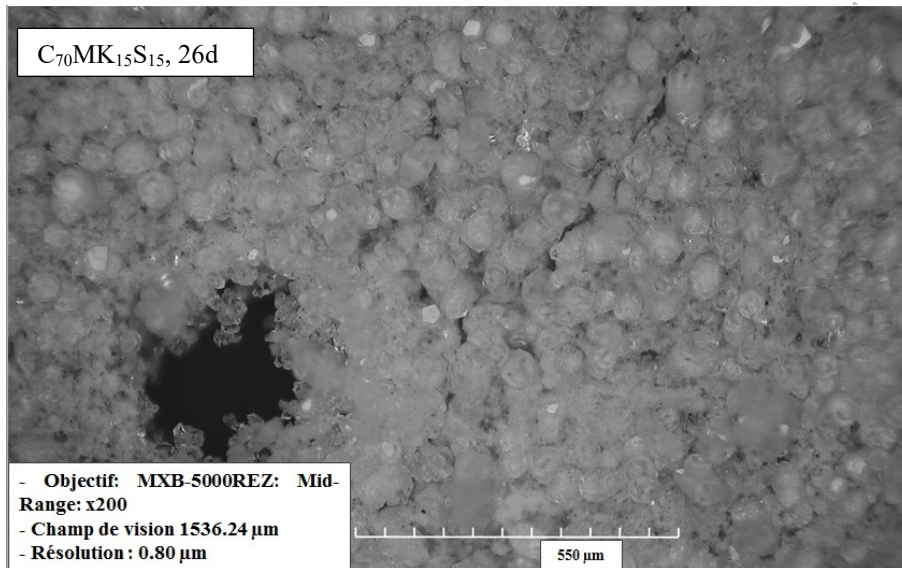
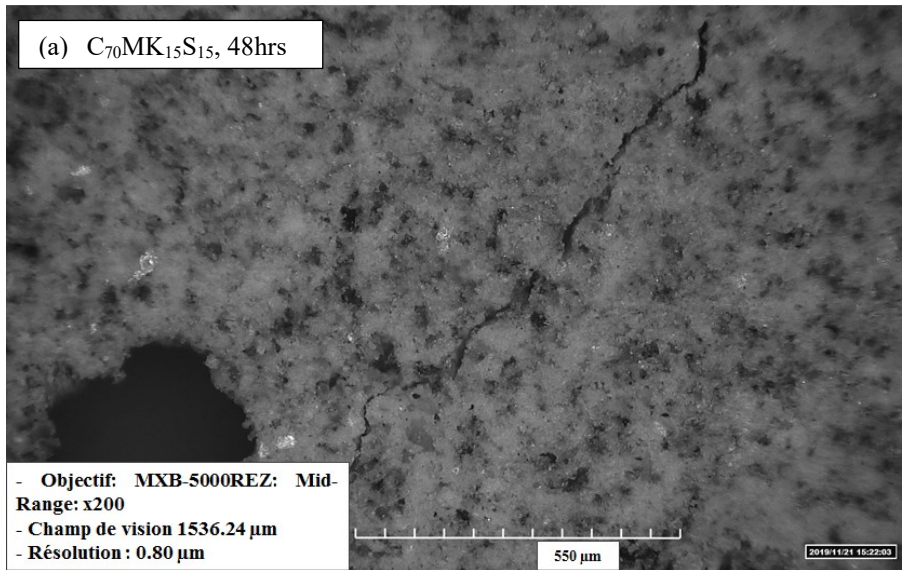
266

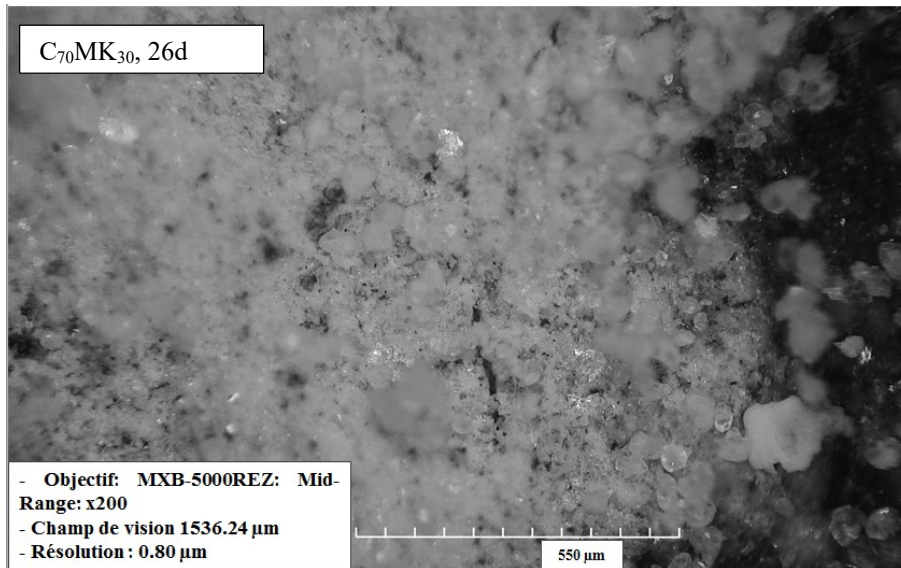
267 **3. Results and discussion**

268 **3.1 2D microscope measurements and SEM/EDX analysis**

269 For the cracked specimens, 2D microscope observations were performed at 48 hours
270 following the three-point-bending tests. After 26 days of healing in water, observations
271 of the precipitation of healing products were done. Fig.4 shows that after self-healing,
272 newly formed reaction products were precipitated in crack, which re-establish the link
273 between the two surfaces of crack. The reaction products are white crystals.

274





275 **Fig.4** 2D microscopic image of specimen with minerals additions before healing (48
 276 hours) and after healing (26 days of immersion in water), (a) for ternary binders
 277 containing 15% of metakaolin and 15% of slag, (b) for binary binders containing 30% of
 278 metakaolin.

279

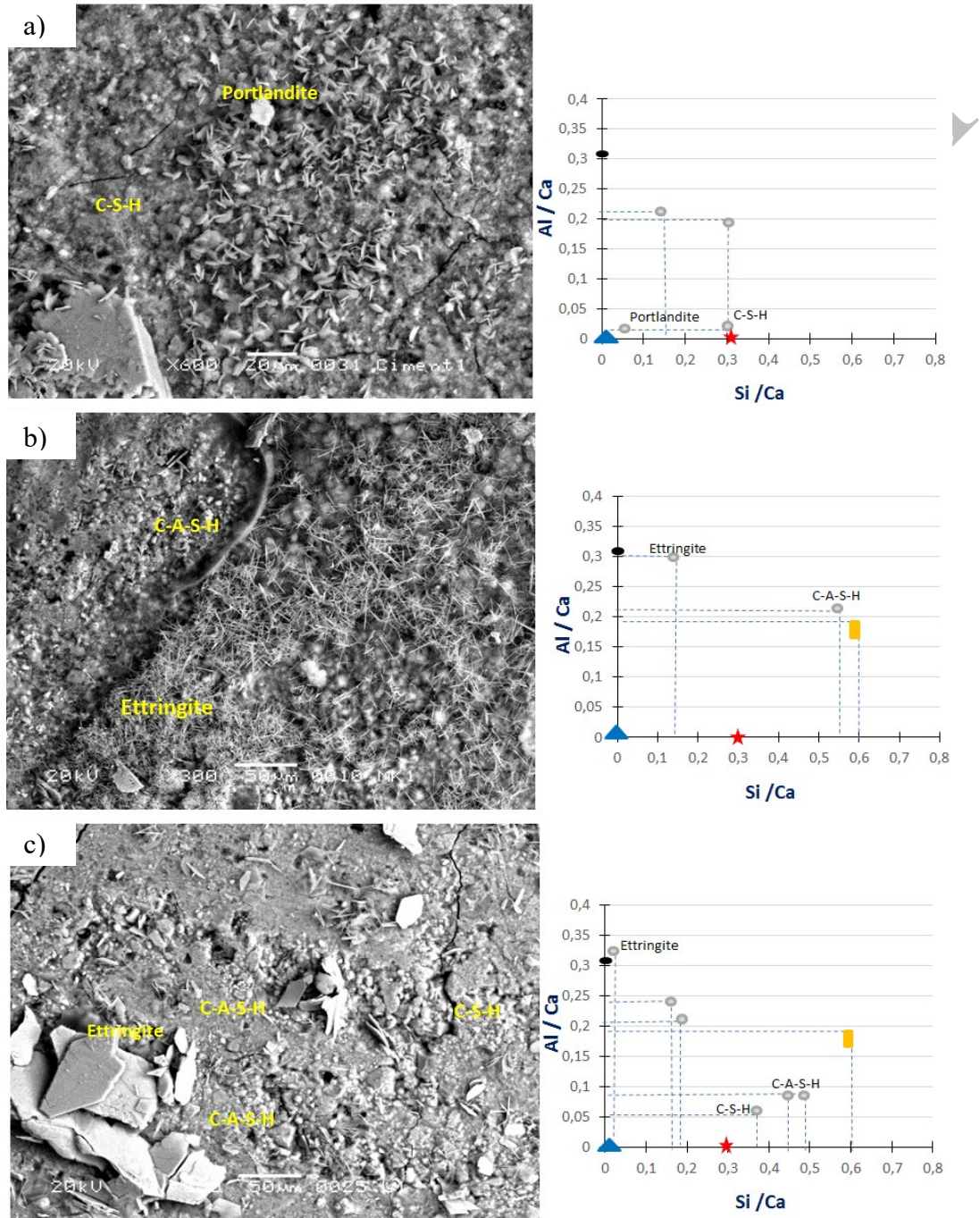
280 Fig.5 illustrates the surface of artificial cracks after self-healing for 26 days. The presence
 281 of ettringite as healing products was commonly found for C₁₀₀, C₇₀MK₃₀ and C₇₀S₃₀. This
 282 product appears due to continuous hydration of unreacted particles of cement.

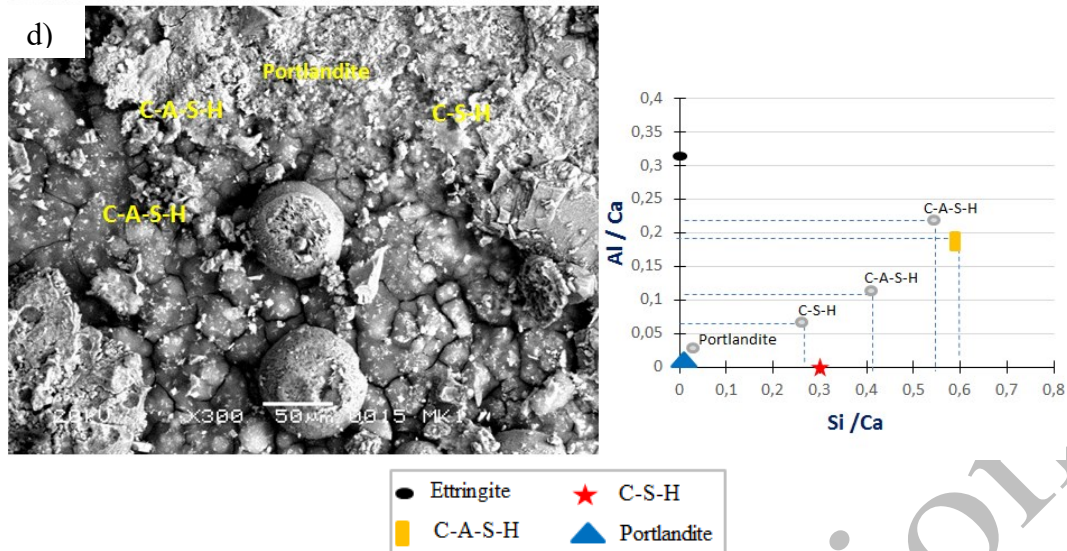
283 Fig.5 shows also the EDS analysis plotted as Al/Ca ratio against of Si/Ca (atomic %). For
 284 binary mixture C₇₀MK₃₀ (Fig.5b), C-A-S-H sheets were detected in addition to the
 285 ettringite as healing products. Metakaolin contains silica and alumina in an active form,
 286 which was assumed to react with portlandite to form C-A-S-H gel [42].

287 As presented in Fig.5d (C₇₀MK₁₅S₁₅), the healing products are most like C-A-S-H. It can
 288 be explained by the pozzolanic reaction of metakaolin and the hydration reaction of slag.

289 From EDX analysis, it was difficult to determine the composition of products due to high
 290 level intermixing with metakaolin, slag, ettringite and C-A-S-H. However, we do not
 291 notice the presence of stralingite, which is also considered as one of the hydration
 292 products of metakaolin [39].

293 Moreover, the healing products as can be seen in Fig.5 c) (C_7S_3O) are most like C-S-H,
 294 ettringite and C-A-S-H. Whenever slag particles are present into contact with portlandite,
 295 their reaction can directly appear by the presence of C-S-H [43]. Therefore, this can lead
 296 to a better self-healing process than that of ordinary mortar mixture.





297
 298 **Fig.5** SEM/EDS analysis of an artificial cracks after 26 days of healing: (a) C₁₀₀, (b)
 299 C₇₀MK₃₀, (c) C₇₀S₃₀, (d) C₇₀MK₁₅S₁₅. Scale bar of BSE images corresponds to 50 μm.
 300 Graphical treatment of EDX points analysis obtained for healed products, Al/Ca ratio is
 301 plotted as a function of Si/Ca ratio (in atomic percentage).

302

303 3.2 TGA analysis

304 Fig.6 illustrates the DTA/DTG profiles of bulk cement paste and healing products formed
 305 in cracks after curing up in water to 26 days. Overall TGA graphs show common
 306 hydration products peaks around 110 °C to 200 °C for hydrates like ettringite, C-S-H gel
 307 [42], [44], around 410 °C to 550 °C for portlandite [45], and the peaks between 660 °C
 308 and 840 °C is mainly due to the decomposition of calcite [46].

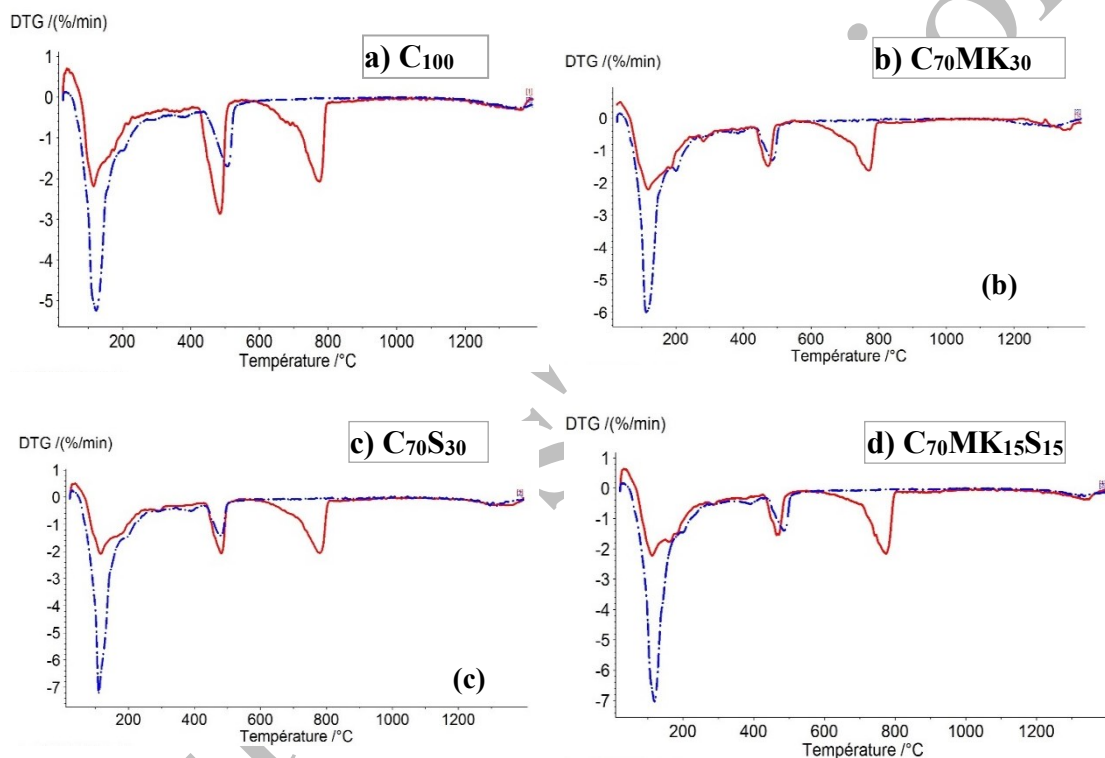
309 For DTG profiles of the healing products for binary and ternary blends (C₇₀MK₃₀,
 310 C₇₀S₃₀ and C₇₀MK₁₅S₁₅), small peaks are observed at about 190-280 °C. They
 311 represent the decomposition of crystalline part of C-A-H, C-A-S-H and the presence of
 312 monocarboaluminate and gehlenite hydrates [42]. Thus, they participate in the
 313 diversification of healing products [47].

314 These phases are formed as results of the pozzolanic reaction of metakaolin with
 315 portlandite that enhances the hydration process. Indeed, a carbonation reaction products
 316 located in cracks evolved rapidly due to the air exposition with a 51% and 70% RH [15],

317 [38]. Moreover, the ingress of CO₂ between each two slices is accelerated by the porous
318 structure of reaction products present between the gaps [15].

319 As shown in Fig.6b and Fig.6c, in the DTG profile of healing products in cracks, the
320 endothermic peak located at 350 °C represents the decomposition of brucite. The presence
321 of brucite as reaction products could be attributed to the presence of Mg in slag
322 composition.

323



324

325 **Fig.6** DTG profiles of cement paste (dashed line) and healing products (continuous line)
326 for the different mixtures.

327

328 3.3 XRD analysis

329 XRD tests were performed to obtain more detailed information about the components of
330 healed products of mixtures containing minerals additions.

331 Fig.7 shows the XRD patterns of the reaction products of self-healing in the specimens
332 continuously immersed in tap water for 26 days. As shown in Fig.7, the reaction products

333 mainly consisted of portlandite and calcite. These products are observed in common for
334 the four different mixtures. In contrast, C-S-H sheets are hardly noticeable by XRD
335 analysis due to their low degree of crystallization. The microstructure of the healing
336 products varies with the chemical composition of minerals additions used. For ordinary
337 C₁₀₀ mixture, the C₂S remains visible after 28 days of aging.

338 In the case where a part of the cement was replaced by metakaolin and slag, XRD patterns
339 indicate that gehlenite, hemicarboaluminate, monocarboaluminate and calcite are formed
340 as reaction products of this combination. Metakaolin hold actively amorphous dioxide
341 and aluminum oxide, they can react with portlandite to form C-S-H, sulfoaluminate and
342 gehlenite [38]. In addition, slag is considered as a pozzolanic material and can react with
343 hydrates of cement (portlandite) to form C-S-H and hydrotalcite [35].

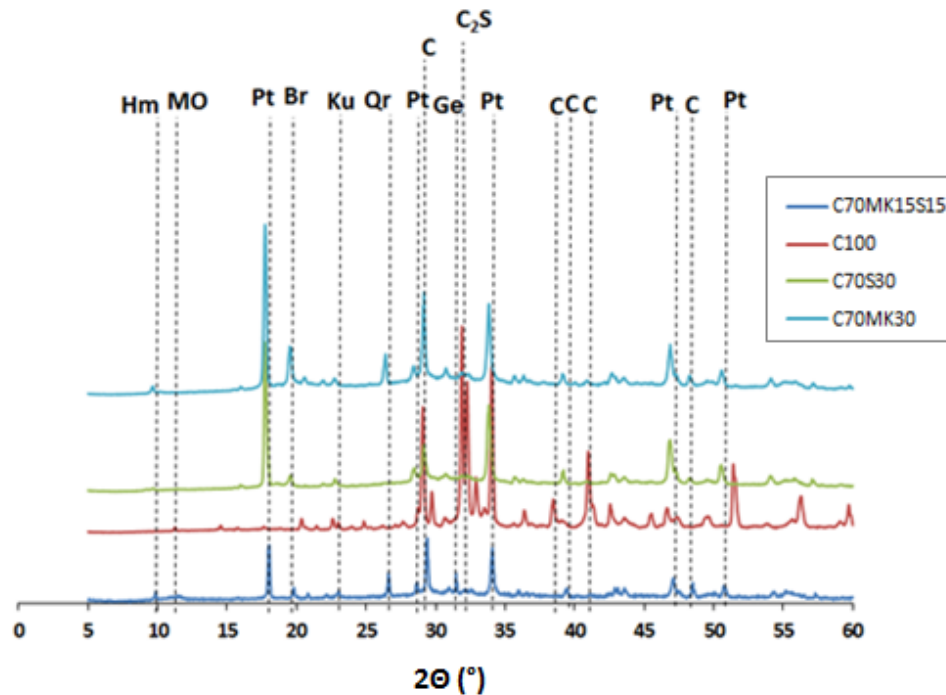
344 It is well known that the lower hydration reaction of slag in comparison to that of cement
345 clinker makes it possible to find, even after years of casting, a large amount of unreacted
346 particles in slag cement paste [15]. Therefore, further reactions of slag particles explain
347 their significant role in self-healing phenomenon [48]. It was confirmed that the self-
348 healing performance was improved when slag that can supply Al ions was incorporated
349 [23], [45]. As reported by many researchers, the complex mechanism reaction of slag
350 leads to a complex mineralogy of healing products in slag cement paste compared to self-
351 healing in Portland cement paste [23]. Moreover, the space factor may also influence the
352 morphology of the reaction products. There is a difference in mineralogy structure of
353 reaction products formed in cracks compared to the hydration products in bulk matrix
354 [10].

355 As indicated in Fig.7, hydrotalcite is not detected as labeled by TGA analyzes for binary
356 mixture that contained slag as a supplementary addition (C₇₀S₃₀). It should be noticed that
357 since the XRD pattern of hydrotalcite is closed to monocarboaluminate, it is possible that

358 monocarboaluminate includes some hydrotalcite that is also considered as reaction
359 products. In $C_{70}MK_{30}$ blend, which contains 30% of MK, there is no trace of stralingite,
360 but the appearance of hydrated calcium aluminate was detected at lines 12° , 26° , 36°
361 and $44^\circ 2\theta$. An increasing value of CH / MK ratio was found more favorable for the
362 production of hydrated calcium aluminates to the detriment of stralingite (C_2ASH_8),
363 which explains the absence of stralingite [49]. The appearance of hydrated calcium
364 aluminates is caused by super saturation of the aqueous phase with respect to CH. High
365 concentrations of Ca^{2+} and OH^- in the pore solution maintained a pore fluid composition
366 that allowed hydrated calcium aluminates to precipitate. XRD data of $C_{70}MK_{30}$ also shows
367 the development of brucite, which is already observed by the DTG analysis of this
368 mixture.

369 By looking at the process of scratching and collecting of healing products, the carbonation
370 of reaction products can take place [35]. Moreover, hemicarboaluminate and
371 monocarboaluminate can be detected when the carbonation of C-A-H takes place
372 especially when reaction products are exposed to air [35], [50]. As discussed above, XRD
373 results of healing products are in agreement with TGA elements detection.

374



375

376 **Fig.7** XRD patterns of healing products formed in cracks created at 2 days and healed for
 377 26 days from single, binary and ternary compositions including slag and metakaolin. HM
 378 (hemicarboaluminate), MO (monocarboaluminate), Pt (portlandite), Br (Brucite), Ku
 379 (kuzelite), Qr (quartz), C (calcite), Ge (gehlenite).

380

381 **3.4 Quantification of mechanical regains due to self-healing**

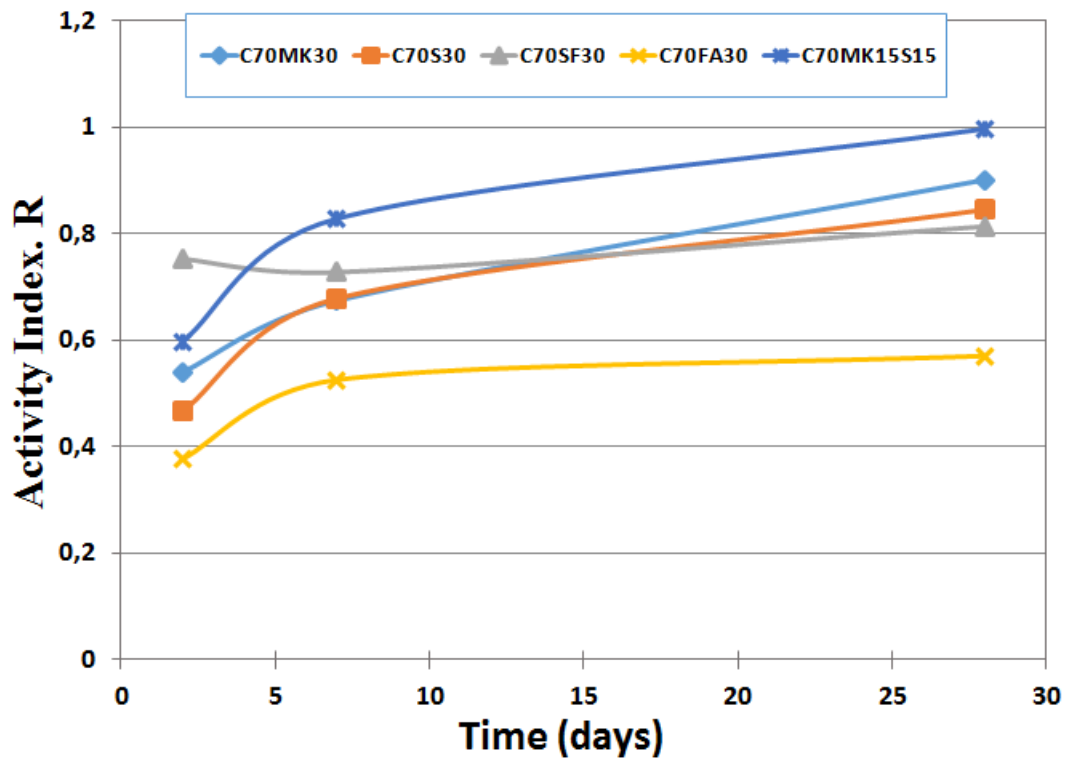
382 In Fig.8 the activity index of SCM mixtures is plotted at different ages: 2, 7 and 28 days.

383 It can be observed that the relative compressive strength significantly varied depending
 384 on the type of SCM.

385 At 2 days, the compressive strength of mortar mixture containing silica fume was higher
 386 than that of ternary composition. At early age, the increase of compressive strength during
 387 the first stage of hydration is attributed to the filler effect. According to the fineness of
 388 silica fume, these results are explained by the filler effect that consists in filling the pore
 389 and thus leading to a denser structure. The lowest rate of compressive strength was
 390 obtained for the mortar sample containing fly ash. Using fly ash shows a reduction in
 391 compressive strength due to low reactivity under ambient conditions [31].

392 Indeed, fly ash is a pozzolanic material that reacts with portlandite of cement matrix and
393 produces C-S-H gel, which contributes in filling the space into cracks. In addition, the
394 benefits added to self-healing ability of cement composites containing fly ash was limited
395 according to CaO content of fly ash [51]. Samson et al. [51] showed that the autogenous
396 healing efficiency was increased when CaO content was high. Otherwise, Hu et al. [29]
397 proved the benefits of combining slag and fly ash on healing properties. The lower
398 reactivity of these two materials compared to cement increases the quantity of unreacted
399 grains and improves the autogenous healing performance.

400 For ternary binder's mixture ($C_{70}MK_{15}S_{15}$), mortar sample developed higher compressive
401 strength than binary mixture containing pure metakaolin or slag ($C_{70}MK_{30}$, $C_{70}S_{30}$)
402 whatever their age. At 28 days, their compressive strength rate was close to sample (C_{100}),
403 confirming that the partial replacement of Portland cement with slag and metakaolin can
404 allow reaching the same compressive strength as ordinary mortar. The highly active
405 pozzolanic reaction of metakaolin with respect to the latent hydraulic properties of slag
406 can explain this balance of functions, which improves compression strength at young age.
407 At early stage of hydration, metakaolin reacts with free lime which leads to reducing the
408 Ca/Si ratio and the pH of internal solution, thus reducing the concentration of hydroxyl
409 ions which are necessary for the hydration phase of slag [43], [52].



410
411 **Fig.8** Activity index for different mixtures (w/b = 0.4)

412 **Fig.9** shows the average force – CMOD curves obtained for beam specimens prepared
413 with different mixtures and subjected to same exposure regime. In this figure, two types
414 of mechanical results are represented:

- 415 - The curves for a cracked specimen and immediately reloaded (test applied on
416 specimen to characterize the mechanical behaviour of specimen without healing
417 process) are included.
- 418 - The reloading curves for healed samples aged 4 weeks in water are also drawn.

419 CMOD of reloading curves are set to 0 in order to have the same initial state, in order to
420 show the effect of mineral additions on mechanical properties after healing process. The
421 recovery in material stiffness is more evident for specimens prepared with the following
422 mixtures: C₇₀MK₁₅S₁₅, C₇₀MK₃₀ and C₇₀S₃₀. We can notice that reloading stiffness tends
423 to be the same as for reference sample. These results indicate that new healing products,

424 with stiffness close to that of primary hydration products, have precipitated in cracks and
425 re-build the link between crack faces.

426 By considering that the reloading part corresponds to the re-opening of the existing crack
427 until the peak load, it is noticeable that there is a brittle damage observed as sharp peak
428 on the graph of $C_{70}SF_{30}$ mixture. We can also notice a variation of stiffness value for the
429 healed specimens of $C_{70}SF_{30}$ (Fig.9 d red curve vs blue curve) caused by the variability
430 of healing, that explain the huge error bar showed in Fig.10. For $C_{70}FA_{30}$, the maximum
431 load obtained was found lower compared to the maximum load for all prepared mortars.
432 It is explained by the reducing of workability of mortar mixture because $C_{70}FA_{30}$ mixture
433 was prepared without adding superplasticizer. The bubbles air of the specimens for this
434 mixture had been observed at the surface of sample. The efficiency of autogenous healing
435 increases with high CaO content [51] [53]. In our work, the fly ash used is Class F (i.e.
436 low calcium content), therefore, it has a very low reactivity. This may explain the limited
437 increase in rigidity of specimens of mortars containing fly ash.

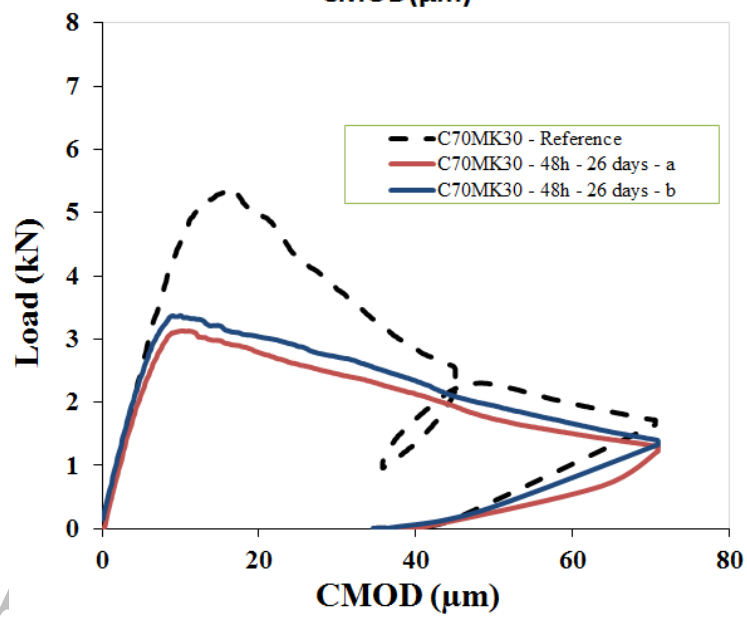
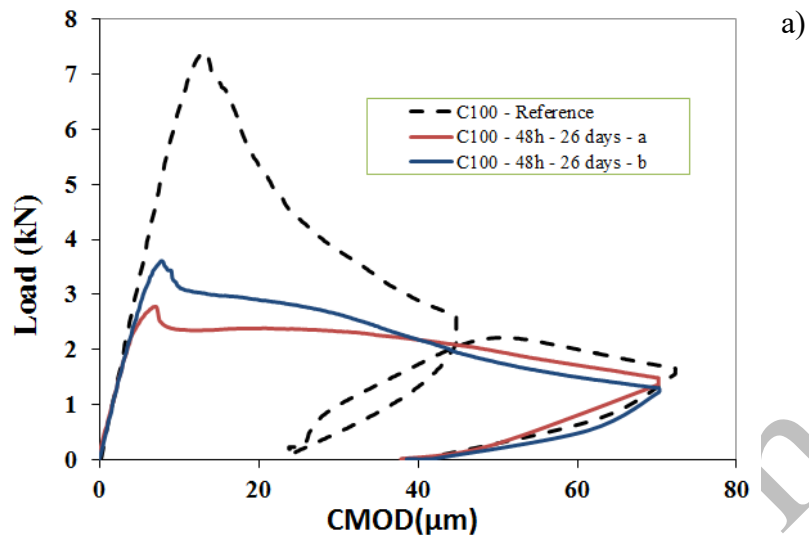
438 The index regains of each mixture test are shown in Fig.10. The strength regains are
439 limited compared to the stiffness regains for all prepared mortars. Likewise, these results
440 have been reported by [13] where a fast recovery of stiffness is noted for specimens
441 cracked at 2 days with a residual crack width of 10 μm . While for the C_{100} samples the
442 amount of stiffness regain is lower than 70%, the other two samples ($C_{70}MK_{30}$ and
443 $C_{70}MK_{15}S_{15}$) containing metakaolin as partial replacement of cement show a higher
444 average stiffness regain ratio (Fig.10). There is a fast recovery by self-healing for samples
445 incorporating 30 vol% metakaolin ($C_{70}MK_{30}$). It can be explained by the highly active
446 pozzolanic reaction of metakaolin with portlandite. Metakaolin reacts with portlandite
447 derived from cement hydration to form additional C-S-H and crystalline products, which

448 contain C_2ASH_8 , C_4AH_{13} and C_3AH_6 . The crystalline products depend mainly on the
449 MK/CH ratio [44], [49].

450 Also Fig.10 highlights that the amount of stiffness regain is much greater compared to
451 others samples due to the presence of slag content with metakaolin. These results can be
452 explained by the fact that both metakaolin and slag are described as active mineral
453 admixtures. They can enhance the mechanical properties and the structure density of
454 cement sample. Generally, the physical effect of these two admixtures is observed when
455 the ultra-fine particles fill the voids and makes the structure denser. The chemical reaction
456 of metakaolin and slag with portlandite produce a dense structure hydration, especially
457 secondary C-S-H phases, which increase the combination force inside the paste matrix,
458 and lead to a higher strength of cement.

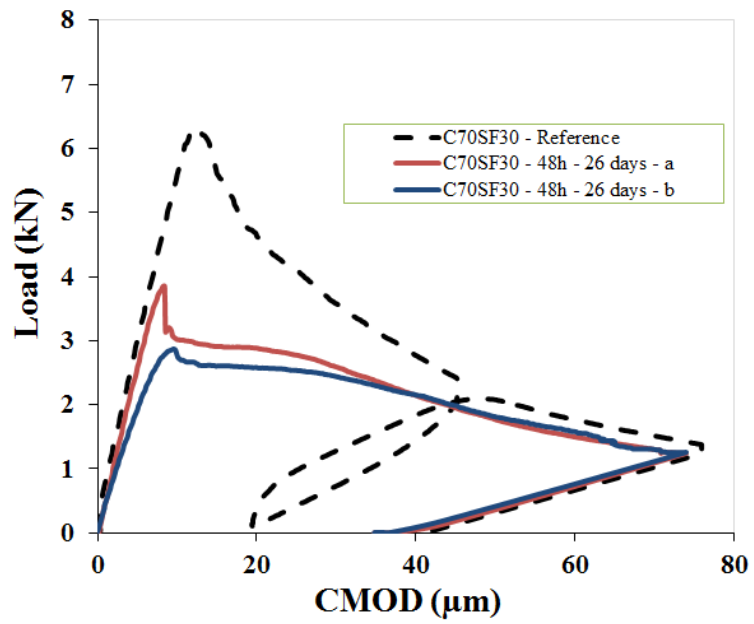
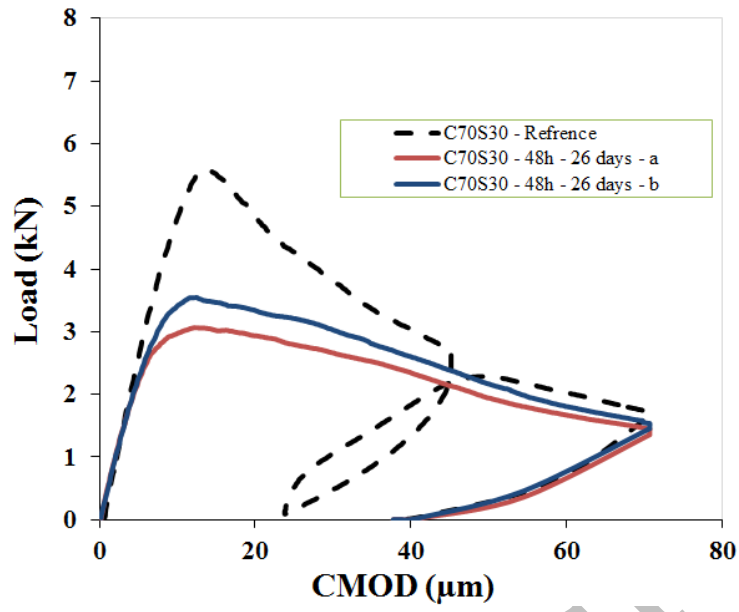
459 It should be noticed that hydration products fill the pore volume because their volume is
460 twice greater than that of anhydrous cement phases, which lead to an increase in bulk
461 density of cement matrix [35]. We can also conclude that the stiffness recovery due to
462 healing by newly formed products is clearly more significant than the strength recovery.
463 It shows that self-healing provides an improvement of rigidity compared to the resistance
464 of healed samples. This can be explained by the fact that the products precipitated re-
465 establish the bond between the two lips of the crack, but do not restore the complex
466 structure that gives its resistance to concrete.

467 When both metakaolin and slag were used at the same time, the chemical phenomenon
468 was called compounding effect [43]. Self-healing with ternary binder provides an
469 improvement of stiffness as compared to cement mortar.



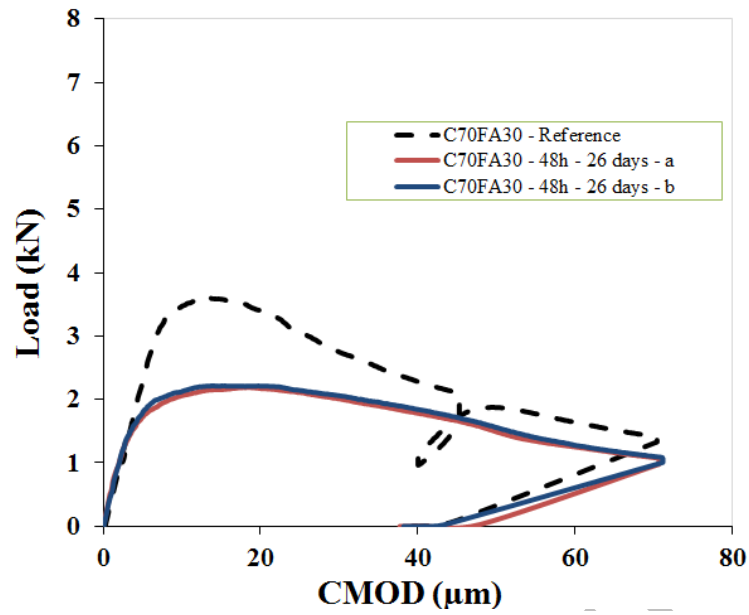
b)

c)

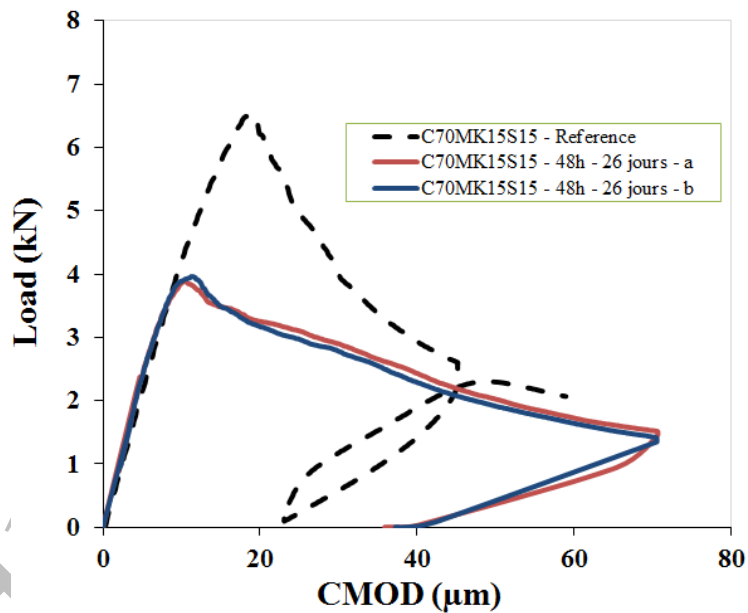


d)

e)

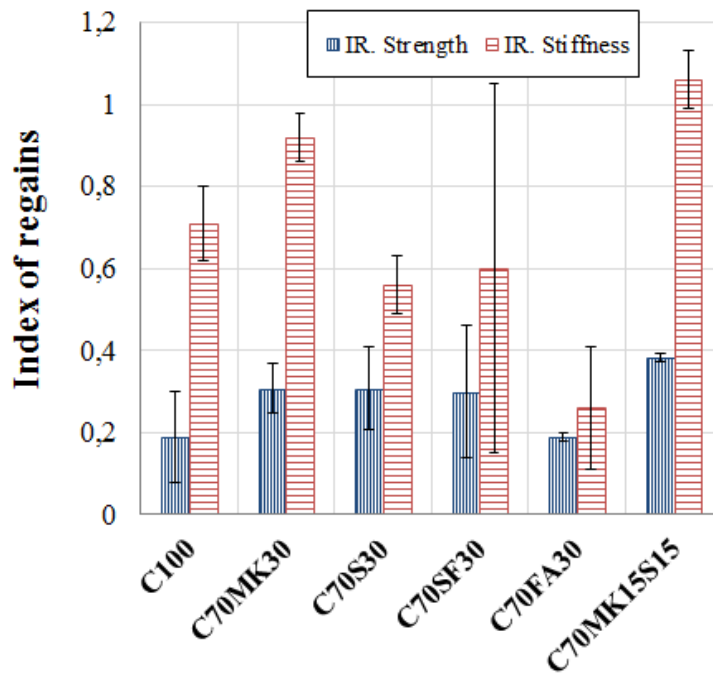


f)



470 **Fig.9** Mechanical behaviour of aged mortar specimens for different SCM's mixtures (load
 471 applied vs. $CMOD$): (a) C_{100} , (b) $C_{70}MK_{30}$, (c) $C_{70}S_{30}$, (d) $C_{70}SF_{30}$, (e) $C_{70}FA_{30}$ and (f)
 472 $C_{70}MK_{15}S_{15}$ (reloading of healed specimens is represented by continuous red/blue curve
 473 while the reference one is represented by a dotted black curve).

474



475 **Fig.10** Effect of different minerals additions on mechanical properties: index of stiffness
 476 and index of strength for healed mortars (10 μ m crack and 26 days of healing). The error
 477 bars indicates the range of standard deviation.
 478

479

480 **4. Conclusion and perspectives**

481 In this study, the extent of self-healing and the chemical composition of self-healing
 482 products of binary and ternary cementitious materials were investigated. Mortar samples
 483 were prepared with a crack width of 10 μ m and healed by water immersion. The
 484 mechanical behaviour of the healed samples was assessed by means of three-point-
 485 bending tests. Besides, artificial cracks were formed in order to characterize the
 486 correspondent self-healing products. SEM/EDS, TGA and XRD tests were carried out to
 487 gain insights into the mineralogical structure of the self-healing products. Based on the
 488 experimental results obtained, conclusions can be drawn as follows:

- 489 - In the case of ternary blends, the self-healing products formed between planar
 490 gaps by continuous hydration were found to be numerous. TGA and XRD results
 491 show newly hydration products precipitates in cracks compared to primary
 492 hydration products (products of bulk paste). The healing products consist of

- 493 monocarboaluminate, hydrotalcite and hemicarboaluminate besides previously
494 reported C-S-H, portlandite and calcite.
- 495 - SEM observations are in agreement with TGA and XRD results as the self-healing
496 products of ternary binders were found very various.
 - 497 - The compressive strength of the ternary composition C₇₀MK₁₅S₁₅ tends to
498 increase progressively to reach approximately the compressive strength of
499 Portland cement-based composition after 28 days of casting.
 - 500 - The partial replacement of cement by metakaolin and slag improves the self-
501 healing efficiency of ternary binders as compared to ordinary formulations. This
502 tendency was shown to be more significant for stiffness than strength probably
503 due to the formation of various products like C-A-S-H phases as well as
504 portlandite and C-S-H gel that make the structure denser.

505
506

Acknowledgments

507 The authors would like to acknowledge Vincent Wisniewski (GeM, Centrale Nantes) for
508 his assistance while performing the experimental tests and Yannick Benoit (GeM,
509 Centrale Nantes) for his technical assistance during SEM/EDX observations. Special
510 thanks are due to Johan Vandendorre for his help in accomplishing XRD tests at Subatech
511 laboratory, IMT Atlantique.

512

References

- 514 [1] K. R. Lauer, "Autogenous healing of cement paste," in *Journal Proceedings*,
515 1956, vol. 52, no. 6, pp. 1083–1098.
- 516 [2] V. C. Li and E.-H. Yang, "Self Healing in Concrete Materials," pp. 161–193,
517 2007.

- 518 [3] K. Van Breugel, “Self-healing concepts in civil engineering for sustainable
519 solutions: potential and constraints,” in *Proceedings of the Second International
520 Conference on Self-Healing Materials*, 2009.
- 521 [4] C. Edvardsen, “Water permeability and autogenous healing of cracks in
522 concrete,” *ACI Mater. J.*, vol. 96, no. 4, pp. 448–454, 1999.
- 523 [5] B. K. R. Lauert and F. Slate, “Autogenous Healing of Cement Paste,” *ACI J.
524 Proc.*, vol. 52, no. 6, pp. 1083–1098, 1956.
- 525 [6] De Rooij, K. van Tittelboom, N. Belie, and E. Schlangen, *Self-Healing
526 Phenomena in Cement-Based Materials: State-of-the-Art Report of RILEM
527 Technical Committee*. 2013.
- 528 [7] D. Fukuda, Y. Nara, D. Hayashi, H. Ogawa, and K. Kaneko, “Influence of
529 fracture width on sealability in high-strength and ultra-low-permeability concrete
530 in seawater,” *Materials (Basel)*, vol. 6, no. 7, pp. 2578–2594, 2013.
- 531 [8] D. Fukuda *et al.*, “Investigation of self-sealing in high-strength and ultra-low-
532 permeability concrete in water using micro-focus X-ray CT,” *Cem. Concr. Res.*,
533 vol. 42, no. 11, pp. 1494–1500, 2012.
- 534 [9] B. Hilloulin, F. Grondin, A. Loukili, and N. De Belie, “Mechanical regains due to
535 self-healing in cementitious materials: Experimental measurements and micro-
536 mechanical model,” *Cem. Concr. Res.*, vol. 80, pp. 21–32, 2015.
- 537 [10] H. Huang, G. Ye, and D. Damidot, “Characterization and quantification of self-
538 healing behaviors of microcracks due to further hydration in cement paste,” *Cem.
539 Concr. Res.*, vol. 52, pp. 71–81, 2013.
- 540 [11] K. Van Tittelboom, E. Gruyaert, H. Rahier, and N. De Belie, “Influence of mix

- 541 composition on the extent of autogenous crack healing by continued hydration or
542 calcium carbonate formation,” *Constr. Build. Mater.*, vol. 37, no. 0, pp. 349–359,
543 2012.
- 544 [12] T. H. Ahn and T. Kishi, “Crack self-healing behavior of cementitious composites
545 incorporating various mineral admixtures,” *J. Adv. Concr. Technol.*, vol. 8, no. 2,
546 pp. 171–186, 2010.
- 547 [13] S. Granger, A. Loukili, G. Pijaudier-Cabot, and G. Chanvillard, “Experimental
548 characterization of the self-healing of cracks in an ultra high performance
549 cementitious material: Mechanical tests and acoustic emission analysis,” *Cem.
550 Concr. Res.*, vol. 37, no. 4, pp. 519–527, 2006.
- 551 [14] Y. Yang, M. D. Lepech, E. H. Yang, and V. C. Li, “Autogenous healing of
552 engineered cementitious composites under wet-dry cycles,” *Cem. Concr. Res.*,
553 vol. 39, no. 5, pp. 382–390, 2009.
- 554 [15] S. Qian, J. Zhou, M. R. de Rooij, E. Schlangen, G. Ye, and K. van Breugel,
555 “Self-healing behavior of strain hardening cementitious composites incorporating
556 local waste materials,” *Cem. Concr. Compos.*, vol. 31, no. 9, pp. 613–621, 2009.
- 557 [16] Y. Yang, E. H. Yang, and V. C. Li, “Autogenous healing of engineered
558 cementitious composites at early age,” *Cem. Concr. Res.*, vol. 41, no. 2, pp. 176–
559 183, 2011.
- 560 [17] S. Jacobsen and E. J. Sellevold, “Self healing of high strength concrete after
561 deterioration by freeze/thaw,” *Cem. Concr. Res.*, vol. 26, no. 1, pp. 55–62, 1996.
- 562 [18] H. Ma, S. Qian, and Z. Zhang, “Effect of self-healing on water permeability and
563 mechanical property of Medium-Early-Strength Engineered Cementitious

- 564 Composites,” *Constr. Build. Mater.*, vol. 68, pp. 92–101, Oct. 2014.
- 565 [19] H. W. Reinhardt and M. Jooss, “Permeability and self-healing of cracked
566 concrete as a function of temperature and crack width,” *Cem. Concr. Res.*, vol.
567 33, no. 7, pp. 981–985, 2003.
- 568 [20] E. Özbay and M. Sahmaran, “Effect of sustained flexural loading on self-healing
569 of engineered cementitious composites,” *J. Adv. Concr. Technol.*, vol. 11, no. 5,
570 pp. 167–179, 2013.
- 571 [21] M. A. A. Sherir, K. M. A. Hossain, and M. Lachemi, “The influence of MgO-
572 type expansive agent incorporated in self-healing system of Engineered
573 cementitious Composites,” *Constr. Build. Mater.*, vol. 149, pp. 164–185, 2017.
- 574 [22] Y. Abdel-Jawad and F. Dehn, “Self-healing of self-compacting concrete,” in
575 *Proceedings of SCC2005 Conference, Orlando, FL, USA, 2005*, pp. 11–15.
- 576 [23] K. Tomczak and J. Jakubowski, “The effects of age, cement content, and healing
577 time on the self-healing ability of high-strength concrete,” *Constr. Build. Mater.*,
578 vol. 187, pp. 149–159, Oct. 2018.
- 579 [24] X. F. Wang *et al.*, “Evaluation of the mechanical performance recovery of self-
580 healing cementitious materials – its methods and future development: A review,”
581 *Constr. Build. Mater.*, vol. 212, pp. 400–421, Jul. 2019.
- 582 [25] K. Olivier, A. Darquennes, F. Benboudjema, and R. Gagné, “Etude de la
583 sensibilité à la fissuration des matériaux cimentaires avec additions minérales au
584 jeune âge,” *31èmes Rencontres de l’AUGC*, 2013.
- 585 [26] A. Darquennes, K. Olivier, F. Benboudjema, and R. Gagné, “Self-healing at
586 early-age, a way to improve the chloride resistance of blast-furnace slag

- 587 cementitious materials,” *Constr. Build. Mater.*, vol. 113, pp. 1017–1028, 2016.
- 588 [27] I. Salama, B. Hilloulin, S. Medjigbodo, and A. Loukili, “Influence of
589 supplementary cementitious materials on the autogenous healing of cracks in
590 cementitious materials,” *ICCM 2017 Montr. ACI Spec. Publ.*, vol. 320, no.
591 October, pp. 12.1-12.14, 2017.
- 592 [28] J. Qiu, H. S. Tan, and E. H. Yang, “Coupled effects of crack width, slag content,
593 and conditioning alkalinity on autogenous healing of engineered cementitious
594 composites,” *Cem. Concr. Compos.*, vol. 73, pp. 203–212, 2016.
- 595 [29] X. Hu, C. Shi, Z. Shi, B. Tong, and D. Wang, “Early age shrinkage and heat of
596 hydration of cement-fly ash-slag ternary blends,” *Constr. Build. Mater.*, vol. 153,
597 pp. 857–865, 2017.
- 598 [30] P. Shen *et al.*, “Experimental investigation on the autogenous shrinkage of steam
599 cured ultra-high performance concrete,” *Constr. Build. Mater.*, vol. 162, pp. 512–
600 522, 2018.
- 601 [31] L. Ferrara and V. Krelani, “A fracture testing based approach to assess the self
602 healing capacity of cementitious composites,” *Proc. 8th Int. Conf. Fract. Mech.*
603 *Concr. Concr. Struct. Fram. 2013*, pp. 351–360, 2013.
- 604 [32] B. Saleh Salem Beshr, I. M. Abdul Mohaimen, M. N. Noor Azline, S. Nor Azizi,
605 A. B. Nabilah, and A. A. Farah Nora Aznieta, “Feasibility assessment on self-
606 healing ability of cementitious composites with MgO,” *J. Build. Eng.*, no. April,
607 p. 101914, 2020.
- 608 [33] G. Yildirim, Ö. K. Keskin, S. B. I. Keskin, M. Şahmaran, and M. Lachemi, “A
609 review of intrinsic self-healing capability of engineered cementitious composites:

- 610 Recovery of transport and mechanical properties,” *Constr. Build. Mater.*, vol.
611 101, pp. 10–21, 2015.
- 612 [34] M. Palou, R. Novotny, D. Všiansky, T. Stane, and M. Bohác, “Investigation on
613 early hydration of ternary Portland cement-blast-furnace slag – metakaolin
614 blends,” vol. 64, pp. 333–341, 2014.
- 615 [35] P. Duan, Z. Shui, W. Chen, and C. Shen, “Enhancing microstructure and
616 durability of concrete from ground granulated blast furnace slag and metakaolin
617 as cement replacement materials,” *J. Mater. Res. Technol.*, vol. 2, no. 1, pp. 52–
618 59, 2013.
- 619 [36] M. A. S. Anjos, A. Camões, P. Campos, G. A. Azeredo, and R. L. S. Ferreira,
620 “Effect of high volume fly ash and metakaolin with and without hydrated lime on
621 the properties of self-compacting concrete,” *J. Build. Eng.*, vol. 27, no. October
622 2019, 2020.
- 623 [37] Y. Kocak, “Effects of metakaolin on the hydration development of Portland–
624 composite cement,” *J. Build. Eng.*, vol. 31, no. April, p. 101419, 2020.
- 625 [38] P. Termkhajornkit, T. Nawa, Y. Yamashiro, and T. Saito, “Self-healing ability of
626 fly ash-cement systems,” *Cem. Concr. Compos.*, vol. 31, no. 3, pp. 195–203,
627 2009.
- 628 [39] M. Sahmaran, G. Yildirim, and T. K. Erdem, “Self-healing capability of
629 cementitious composites incorporating different supplementary cementitious
630 materials,” *Cem. Concr. Compos.*, vol. 35, no. 1, pp. 89–101, 2013.
- 631 [40] M. Mohammadi, C. Youssef-Namnoum, M. Robira, and B. Hilloulin, “Self-
632 Healing Potential and Phase Evolution Characterization of Ternary Cement

- 633 Blends,” *Materials (Basel, Switzerland)*, vol. 13, no. 11. Institut de Recherche en
634 Génie Civil et Mécanique (GeM), UMR 6183, Ecole Centrale de Nantes-
635 Université de Nantes-CNRS, 1 rue de la Noë, 44321 Nantes, France., 2020.
- 636 [41] B. Hilloulin, “Analyse croisée et modélisation multi-échelle de l’auto-
637 cicatrisation des matériaux cimentaires,” pp. 1–8, 2015.
- 638 [42] H. El-Diadamony, A. A. Amer, T. M. Sokkary, and S. El-Hoseny, “Hydration
639 and characteristics of metakaolin pozzolanic cement pastes,” *HBRC J.*, vol. 14,
640 no. 2, pp. 150–158, 2018.
- 641 [43] Z. Li and Z. Ding, “Property improvement of Portland cement by incorporating
642 with metakaolin and slag,” *Cem. Concr. Res.*, vol. 33, no. 4, pp. 579–584, 2003.
- 643 [44] J. M. Kinuthia, S. Wild, B. B. Sabir, and J. Bai, “Self-compensating autogenous
644 shrinkage in Portland cement—metakaolin—fly ash pastes,” *Adv. Cem. Res.*, vol.
645 12, no. 1, pp. 35–43, Jan. 2000.
- 646 [45] L. P. Esteves, “On the hydration of water-entrained cement-silica systems:
647 Combined SEM, XRD and thermal analysis in cement pastes,” *Thermochim.*
648 *Acta*, vol. 518, no. 1–2, pp. 27–35, 2011.
- 649 [46] I. Halikia, L. Zoumpoulakis, E. Christodoulou, and D. Prattis, “Kinetic study of
650 the thermal decomposition of calcium carbonate by isothermal methods of
651 analysis,” *Eur. J. Miner. Process. Environ. Prot.*, vol. 1, no. 2, pp. 89–102, 2001.
- 652 [47] O. Chowaniec, “Limestone Addition in Cement, Ph.D. Thesis, EPFL,” vol. 5335,
653 2012.
- 654 [48] P. Byoungsun and C. C. Young, “Investigating a new method to assess the self-
655 healing performance of hardened cement pastes containing supplementary

- 656 cementitious materials and crystalline admixtures,” *J. Mater. Res. Technol.*, vol.
657 8, no. 6, pp. 6058–6073, Nov. 2019.
- 658 [49] M. Murat, “Hydration reaction and hardening of calcined clays and related
659 minerals. II. Influence of mineralogical properties of the raw-kaolinite on the
660 reactivity of metakaolinite,” *Cem. Concr. Res.*, vol. 13, no. 4, pp. 511–518, 1983.
- 661 [50] D. Damidot and F. P. Glasser, “Thermodynamic investigation of the CaO—
662 Al₂O₃—CaSO₄—CaCO₃-H₂O closed system at 25°C and the influence of
663 Na₂O,” *Cem. Concr. Res.*, vol. 27, no. 3, pp. 129–134, 1994.
- 664 [51] G. Samson, M. Cyr, and X. X. Gao, “Formulation and characterization of
665 blended alkali-activated materials based on flash-calcined metakaolin, fly ash and
666 GGBS,” *Constr. Build. Mater.*, vol. 144, pp. 50–64, 2017.
- 667 [52] J. M. Khatib and J. J. Hibbert, “Selected engineering properties of concrete
668 incorporating slag and metakaolin,” *Constr. Build. Mater.*, vol. 19, pp. 460–472,
669 2005.
- 670 [53] M. Şahmaran, S. B. Keskin, G. Ozerkan, and I. O. Yaman, “Self-healing of
671 mechanically-loaded self consolidating concretes with high volumes of fly ash,”
672 *Cem. Concr. Compos.*, vol. 30, no. 10, pp. 872–879, 2008.

673